ELSEVIER

Journal of Crystal Growth 184/185 (1998) 223–227

JOURNAL OF CRYSTAL GROWTH

Investigation of the surfactant effect of Sn in ZnSe by reflectance difference spectroscopy and reflection high-energy electron diffraction

H.D. Jung[a], N. Kumagai[a], T. Hanada[a], E. Kurtz[a], Z. Zhu[a], T. Yao[a,b,*]

[a] *Institute for Materials Research, Tohoku University, Sendai 980-77, Japan*
[b] *Joint Research Center for Atom Technology, Tsukuba, Ibaraki 305, Japan*

Abstract

We have studied the surfactant effect of Sn on ZnSe(0 0 1) growth by molecular beam epitaxy equipped with in-situ reflection high-energy electron diffraction and reflectance difference spectroscopy and in-line Auger electron spectroscopy. Sn deposited on the Zn stabilized $c(2\times2)$ ZnSe surface showed surface segregation, while Sn deposited on the Se-stabilized (2×1) surface does not segregate to the growing surface. We have demonstrated that Sn deposited on the Zn stabilized ZnSe surface improve two-dimensional growth in highly strained CdSe/ZnSe system.

PACS: 83.70; 81.10; 81.05.E

Keywords: ZnSe; MBE; Surfactant; RHEED; RDS; Quantum structure

1. Introduction

Recent investigations of the fabrication of self-organized low-dimensional quantum structures suggest that the control of surface energy and growth kinetics are crucial to obtain well-defined quantum structures, since the surface processes during epitaxy are dominated by these two factors. The surface energetics and growth kinetics can be controlled by employing surfactant mediated-molecular beam epitaxy (SM-MBE), in which surfactant atoms of one monolayer (ML) thickness are predeposited onto a substrate surface prior to growth. As the epitaxy proceeds, the surfactant atoms segregate to the growing surface which affects either the surface energy or growth kinetics. The SM-MBE has been well studied for GaAs and Ge/Si systems [1–6]. The surfactant atom either enhances migration of adatoms (i.e. nonreactive surfactant) by reducing the surface energy, or decreases the migration length of adatoms (i.e. reactive surfactant) through an increase in nucleation

* Corresponding author. Fax: +81 22 215 2073; e-mail: yao@imr.tohoku.ac.jp.

0022-0248/98/$19.00
PII S0022-0248(97)00681-7

sites. An example of the former type of surfactant is Sn in homoepitaxy of GaAs [1,2], while the latter type surfactant atom includes Te in heteroepitaxial growth of InGaAs on GaAs [3–6].

So far, there has been no report on the SM-MBE of II–VI compounds. This paper presents the first report on the SM-MBE growth of II–VI compounds. We have investigated in situ the behaviors of Sn atoms predeposited onto ZnSe surfaces during ZnSe epitaxy by reflectance difference spectroscopy (RDS), reflection high-energy electron diffraction (RHEED), and Auger electron spectroscopy (AES). We have found that Sn indeed acts as surfactant when predeposited onto the Zn-stabilized $c(2\times2)$ ZnSe surface, while no segregation of Sn to the surface was observed when deposited onto the Se-stabilized (2×1) surface. We have further investigated the role of Sn during heteroepitaxy of CdSe on ZnSe, where the lattice misfit is 8%. It is found that CdSe grows in a layer by layer growth mode from the very beginning of heteroepitaxy in the SM-MBE, while three-dimensional (3D) island growth dominates in the conventional MBE growth.

2. Experimental procedure

Experiments have been performed in a solid source MBE equipped with in situ RDS and RHEED and in-line AES. The RDS setup used in the present experiments was similar to the one developed by Aspnes et al. [7]. RDS measures the optical anisotropy between two optical axes ([1 $\bar{1}$ 0] and [1 1 0]) and is known to be a powerful tool for probing local changes of the surface in materials with isotropic bulk properties such as (0 0 1)GaAs and ZnSe [7–10]. Since the surface optical response reflects the electronic structure, RDS is complementary to RHEED which relies on the long-range order of the surface.

A ZnSe buffer layer was grown on a semi-insulating (0 0 1)GaAs substrate at a substrate temperature of 300°C with the beam flux ratio of Se to Zn being adjusted to obtain a (2×1) and $c(2\times2)$ mixed RHEED pattern and a growth rate of 300 nm/h. 0.5–1.5 MLs of Sn were evaporated onto ZnSe surfaces with different surface chemistry at the same substrate temperature. The deposited Sn was quantitatively analyzed by AES.

We have investigated the behaviors of Sn during ZnSe epitaxy on a ZnSe buffer layer and heteroepitaxy of CdSe on ZnSe. In the former experiment, Sn was deposited either onto the Se stabilized (2×1) ZnSe surface or onto the Zn stabilized $c(2\times2)$ surface. The Zn-stabilized surface was prepared by exposing the surface of the ZnSe buffer layer with Zn. Since the desorption of Se from the ZnSe surface was not neglected at a substrate temperature of 300°C, Se in addition to Sn was deposited onto the surface to preserve (2×1) reconstruction. The growth of ZnSe resumed on the Sn-deposited surfaces either by atomic layer epitaxy (ALE) or MBE. The growth process was assessed by RHEED and RDS, and surface composition analysis was done by AES. In heteroepitaxy of CdSe on ZnSe, CdSe was grown on a Sn-treated ZnSe surface and was compared with the growth of CdSe by conventional MBE. We have investigated the surface morphology of the layers by atomic force microscopy (AFM) and the optical properties by photoluminescence (PL) spectroscopy.

3. The effect of surface chemistry on the role of Sn in ZnSe growth

3.1. Predeposited Sn layer onto the Zn-stabilized surface

The dashed curve in Fig. 1a shows a RD spectrum of a Se-exposed (2×1) surface (designated as Se/ZnSe) which is characterized by a peak at around 5 eV, while that of a Zn-exposed $c(2\times2)$ surface (designated as Zn/ZnSe) showed a dip around the same energy [10]. We note that E_1 critical point is located close to 5 eV. On exposing 1 ML thick Sn on the Zn-stabilized $c(2\times2)$ surface, the RD spectrum immediately changed to the dotted curve ($X=0$) which shows a broad dip around 5 eV and a broad peak at around 3.3 eV. It should be noted that this RD spectrum was taken under the Se beam after the deposition of the Sn layer. The evolution of RD spectra taken under the Se beam after each ALE cycle for ZnSe growth on

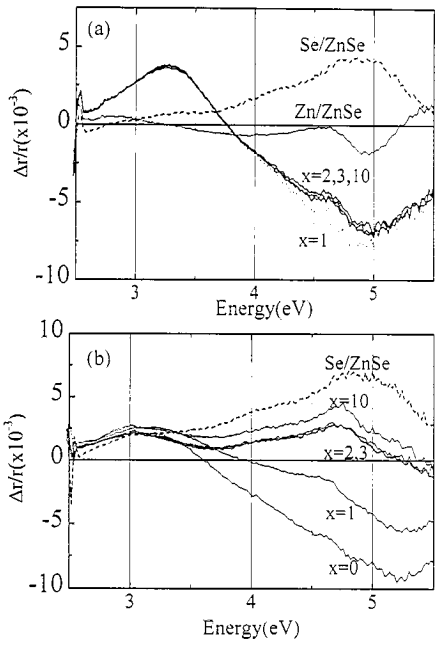

Fig. 1. RD spectra of a Se stabilized ZnSe surface before (dashed line) and after Sn deposition for several ALE cycles (x = 1, 2, 3, 10) ZnSe overgrowth. Sn was deposited on an initially Zn-terminated surface (a) and on a Se terminated surface (b). Thin solid line in (a) shows the RD spectrum for a Zn stabilized ZnSe surface before Sn deposition.

the Sn-predeposited ZnSe buffer layer can be seen in this figure. The x value designates the number of ALE cycles. Surprisingly, the essential features of RD spectra did not change from that of the Sn-predeposited ZnSe surface even with an increase in ALE cycle upto 10. We noted that a further increase in ALE cycle, indeed, did not make an essential change in RD spectrum. These results suggest the segregation of Sn to the growing surface.

The segregation of Sn is clearly indicated by AES measurements as shown in Fig. 2a. This spectrum was taken on a 20 nm thick ZnSe grown on a Sn-predeposited ZnSe buffer layer by MBE. Sn is clearly detected together with Zn and Se with almost the same intensity. The concentration of Sn is estimated to be 0.85 ML.

The evolution of RHEED pattern during the ALE process was quite interesting. Deposition of more than 0.5 ML of Sn onto the Zn-stabilized surface changed the surface reconstruction from

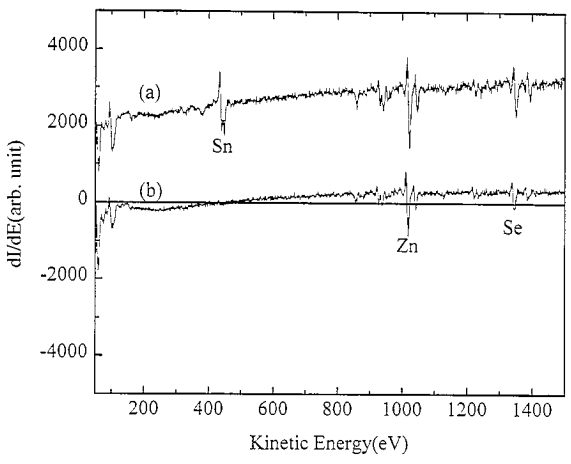

Fig. 2. AES results obtained from the ZnSe surface after MBE growth of 20 nm thick ZnSe layer following Sn (1 ML) predeposition on a Zn-stabilized surface (a) and on a Se-stabilized surface(b).

$c(2\times2)$ to (2×1). The (2×1) pattern was observed throughout the opening and closing cycle of the Se shutter. This is in contrast to a conventional ALE cycle without a pre-deposited Sn layer, where the (2×1) pattern changes to $c(2\times2)$ due to desorption of Se from the surface [11]. On impinging the Zn beam onto the (2×1) reconstructed surface, the RHEED pattern changed to (1×1), which was taken over by (2×1) reconstruction on closing the Zn shutter. This evolution of RHEED pattern suggests that a 2D growth proceeds in surfactant mediated ALE growth. It could be suggested that the (2×1) reconstruction which appeared both after deposition of Sn and on closing the Se and Zn shutters be ascribed to a Sn-induced surface reconstruction.

3.2. Predeposited Sn layer onto Se-stabilized ZnSe surface

The dotted curve in Fig. 1b shows RD spectrum of a Sn predeposited layer on the Se-stabilized ZnSe buffer layer. All RD spectra were taken under the Se beam. The feature of this RD spectrum is almost the same as that of a Sn predeposited layer on the Zn-stabilized ZnSe (dotted curve in Fig. 1a) except the position of the dip: the dip position in Fig. 1a is around 4.9 eV, while that in Fig. 1b is

5.2 eV. With increase in ALE cycle the dip at around 5.2 eV is reduced in intensity and eventually changes to a peak located at 4.8 eV which corresponds to the peak position of the RD spectrum from the Se-stabilized ZnSe surface (see dashed curve in Fig. 1b). The intensity of the 4.8 eV peak gradually increases with increase in ALE cycle. Moreover the general feature of the RD spectra tend to converge to the RD spectrum from the Se-stabilized ZnSe surface. These results are in contrast to the case of Fig. 1a and suggest that Sn does not segregate onto the growing surface. This discussion is substantiated by AES data as shown in Fig. 2b. The sample here is a 20 nm thick ZnSe grown on a Sn-predeposited buffer layer by MBE, where the surface of the buffer layer was Se-stabilized one. No trace of Sn was detected by AES, while Zn and Se were detected with reasonable intensity, indicating that Sn does not segregate to the surface.

The evolution of RHEED during the ALE cycle at the very beginning showed quite different features from the previous case as described in Section 3.1 only when the Zn shutter was closed. The Sn predeposited layer on the Se-stabilized buffer layer showed (2×1) reconstruction which was preserved during the opening and closing periods of Se. On opening the Zn shutter, the (2×1) reconstruction changed to (1×1) pattern and this pattern is preserved during closing period of the Zn shutter. This feature could be understood, if one assumes that the (2×1) reconstruction is associated with the surface Sn and that Sn does not segregate to the growing surface. However, it should be noted that a close observation of RHEED pattern indicates degradation to a spotty pattern as the growth proceeds which suggest onset of 3D island growth.

4. Heteroepitaxial growth of CdSe on ZnSe

The effect of Sn predeposition on heteroepitaxial growth of CdSe on ZnSe has been investigated. CdSe layers were grown by ALE with three ALE cycles on a thick ZnSe buffer layer followed by the growth of a capping 20 nm thick ZnSe layer. Other CdSe layers with nominally equivalent thickness were grown on top of the ZnSe cap layer by ALE. In this experiment, two kinds of ZnSe buffer layers were prepared: a Sn-predeposited ZnSe layer on the Zn-stabilized surface and a ZnSe layer with the Se-stabilized ZnSe surface. Fig. 3a and Fig. 3b show AFM images of CdSe grown (a) with and (b) without the Sn interlayer. Quite big difference in growth mode can be observed for the two cases. In the case of surfactant ALE growth of CdSe, a wavy

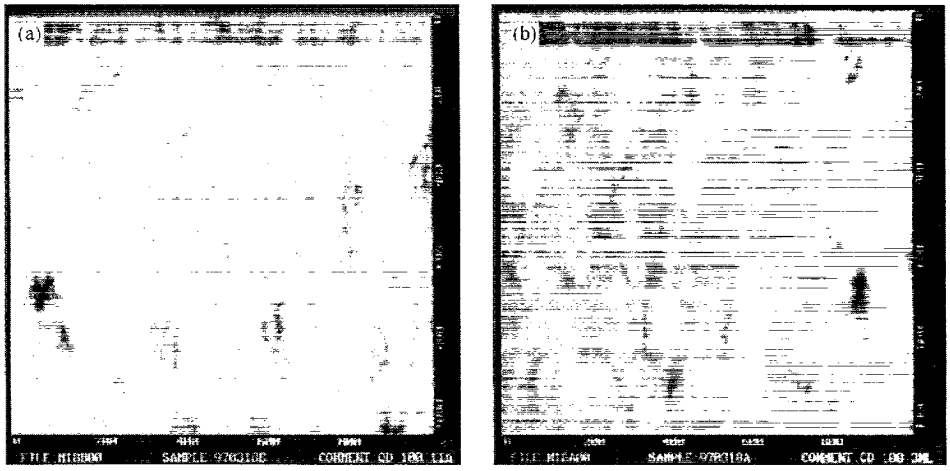

Fig. 3. AFM results for three ALE cycles of CdSe on ZnSe. The structure is as follows: (from surface to substrate) (a) CdSe (3ALE)/ZnSe (20 nm)/CdSe (3ALE)/ZnSe (3ALE)/Sn (0.6 ML)/Zn-terminated ZnSe (~1000 nm)/substrate; (b) CdSe (3ALE)/ZnSe (200A)/CdSe (3ALE)/ZnSe (~1000 nm)/substrate.

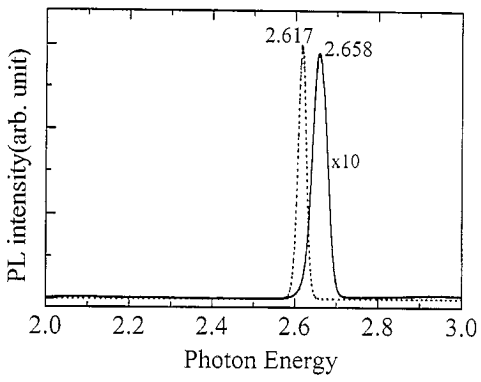

Fig. 4. PL results for the structures of Fig. 3a (solid line) and of Fig. 3b (dotted line).

surface morphology is observed suggesting the formation of quantum well structures, while dot structures are clearly observed in the case of conventional ALE growth of CdSe. Similar dot structure has been observed most recently [12].

The formation of the quantum well structures and dot structures are evidenced by PL measurements (Fig. 4). The PL of both samples are dominated by the near band emission (presumably due to excitonic emission) located at 2.658 eV for the surfactant ALE CdSe QW (solid line) and 2.617 eV for the CdSe quantum dots (dotted line). The peak energy for the quantum dots is shifted to the low-energy side by 0.041 eV, which could be interpreted if one considers the difference in thickness of both quantum structures. However, as suggested through extensive PL study [13], alloying effects presumably proceed during growth and the proper interpretation needs more detailed study.

As the surface migration increases, 3D clusters are more easily formed, while 2D nucleation and growth dominates when the migration length is reasonably short. Hence, the striking difference in growth of CdSe on ZnSe with and without Sn interlayer suggests that Sn reduces the migration of adatoms through increasing nucleation sites.

5. Conclusions

We have demonstrated by means of in situ RHEED, RDS and in-line AES that Sn segregates to the growing surface of ZnSe and CdSe/ZnSe if it is initially deposited on a Zn terminated ZnSe surface. AFM and PL results show that Sn deposited on the Zn stabilized ZnSe surface promotes 2D growth for a highly strained layer system CdSe/ZnSe with results of AFM and PL measurements.

Acknowledgements

H.D. Jung would like to thank Dr. T. Yasuda and Dr. K. Kimura of JRCAT for valuable discussion and continuous encouragement.

References

[1] G.S. Petrich, A.M. Dabiran, P.I. Cohen, Appl. Phys. Lett. 61 (1992) 162.
[2] J.J. Harris, D.E. Ashenford, C.T. Foxon, P.J. Dobson, B.A. Joyce, Appl. Phys. A 33 (1984) 87.
[3] E. Tournie, K.H. Ploog, Thin Solid Films 231 (1993) 43.
[4] J. Massies, N. Grandjean, V.H. Etgens, Appl. Phys. Lett. 61 (1992) 99.
[5] E. Tournie, N. Grandjean, A. Trampert, J. Massies, K.H. Ploog, J. Crystal Growth 150 (1995) 460.
[6] M. Copel, M.C. Reuter, E. Kaxiras, R.M. Tromp, Phys. Rev. Lett. 63 (1989) 632.
[7] D.E. Aspnes, J.P. Harbison, A.A. Studna, L.T. Florez, J. Vac. Sci. Technol. A 6 (1988) 1327.
[8] I. Kamiya, D.E. Aspnes, L.T. Florez, J.P. Harbison, Phys. Rev. B 46 (1992) 15894.
[9] T. Yasuda, K. Kimura, S. Miwa, L.H. Kuo, C.G. Jin, K. Tanaka, T. Yao, Phys. Rev. Lett. 77 (1996) 326.
[10] J.-T. Zettler, K. Stahrenberg, W. Richter, H. Wenisch, B. Jobst, D. Hommel, J. Vac. Sci. Technol. B 14 (1996) 2757.
[11] T. Yao, T. Takeda, Appl. Phys. Lett. 48 (1986) 160.
[12] S.H. Xin, P.D. Wang, Aie Yin, C. Kim, M. Dobrowolska, J.L. Merz, J.K. Furdyna, Appl. Phys. Lett. 69 (1996) 3884.
[13] Z. Zhu, H. Yoshihara, K. Takebayashi, T. Yao, J. Crystal Growth 138 (1994) 619.